

1 **Water dispersible colloids and related nutrient availability in**
2 **Amazonian Terra Preta soils**

3

4 Qian Zhang^{1,2}, Roland Bol¹, Wulf Amelung^{1,3}, Anna Missong¹, Jan Siemens⁴, Ines Mulder⁴,
5 Sabine Willbold⁵, Christoph Müller^{6,7}, Aleksander Westphal Muniz⁸ and Erwin Klumpp¹

6 1. Institute of Bio- and Geosciences, Agrosphere (IBG-3), Forschungszentrum Jülich
7 GmbH, Wilhelm-Johnen-Str., 52425 Jülich, Germany

8 2. Institute for Environmental Research, Biology 5, RWTH Aachen University,
9 Worringerweg 1, 52074 Aachen, Germany

10 3. Institute of Crop Science and Resource Conservation, Soil Science and Soil Ecology,
11 University of Bonn, Bonn, Germany

12 4. Institute of Soil Science and Soil Conservation, iFZ Research Centre for Biosystems,
13 Land Use and Nutrition, Justus Liebig University Giessen, Heinrich-Buff-Ring 26–32,
14 35392 Giessen, Germany

15 5. Central Institute for Engineering, Electronics and Analytics, Analytics (ZEA-3),
16 Forschungszentrum Jülich GmbH, Wilhelm-Johnen-Str., 52425 Jülich, Germany

17 6. Institute of Plant Ecology, Justus Liebig University Giessen, Heinrich-Buff-Ring 26,
18 Giessen 35392, Germany

19 7. School of Biology and Environmental Science and Earth Institute, University College
20 Dublin, Dublin, Ireland

21 8. Embrapa Amazônia Ocidental, Empresa Brasileira de Pesquisa Agropecuária, AM 010
22 Road, km 29, Manaus 69010970, Brazil
23 Corresponding author: q.zhang@fz-juelich.de
24 Key word: Amazonian dark earth, soil colloids, phosphorus, nutrient retention,
25 asymmetric flow field-flow fractionation, ^{31}P -NMR
26

27 Abstract

28 Amazonian Dark Earths (or terra preta de índico) are known as highly fertile soils that can
29 maintain elevated crop yields for centuries. While this fertility was frequently ascribed to
30 the presence of black carbon, the availability and colloidal binding of major nutrients
31 received limited attention. We examined the size distribution and the elemental
32 compositions of water-dispersible colloids (WDC) in both forested and cultivated Terra
33 Preta topsoils (0-10 cm, Anthrosols), as well as in their adjacent non-Terra Preta controls
34 (Acrisols) via asymmetric flow field-flow fractionation (FFF). Liquid-state ^{31}P -nuclear
35 magnetic resonance (NMR) spectra, black carbon content, and scanning electron
36 microscope (SEM) images were also obtained. We found that WDC in Terra Preta soils
37 contained a significant proportion of organo-mineral associations in the size range 30-300
38 nm, whereas, in contrast, water-dispersible nanoparticles with a diameter $<30\text{nm}$ were
39 dominant in the adjacent Acrisols. The shifts to larger WDC sizes in the Terra Preta soils
40 went along with elevated pH values, as well as with elevated contents of Si, Al, Fe, Ca and
41 organic matter-containing particles. Also P concentrations were enriched in both the water-
42 extractable phase (WEP) and WDC extracts of Terra Preta soils relative to the adjacent
43 Acrisols. We assume that the higher pH values and Ca ion concentrations promoted the
44 involvement of soil organic matter (SOM) into the formation of larger-sized colloids
45 consisting of kaolinite-like clay minerals, iron oxides and Ca ions in the Terra Preta soils.
46 The elevated content of Ca in Terra Preta soil colloids may also contribute to the retention
47 of P, likely via bridging of anionic P like orthophosphate to SOM. Preventing soil
48 acidification is thus not only to be recommended for Acrisols, but also for maintaining
49 colloidal structures and related fertility in Terra Preta soils.

1. Introduction

Patches of dark-coloured soils, commonly referred to as Amazonian Dark Earths (ADE) or by their local name terra preta de índico (Terra Preta in short) are increasingly discovered in the Amazon basin. In contrast to the reddish to yellowish colored, highly weathered Ferralsols and Acrisols, the Terra Preta soils owe their characteristic black color likely to their elevated charcoal contents (Sombroek et al., 2004). As a result, much of the fertility of Terra Preta soils was ascribed to the presence of black carbon (Atkinson et al., 2010; Oliveira et al., 2018; Steiner et al., 2007), while the availability and bonding forms of nutrients have received less attention.

The earliest Terra Preta related publications can be traced back to 1874 by the geologist Charles Hartt; since then the number of publications rose considerably, particularly since the early 1990s (Woods and Denevan, 2009). One main reason is that the Terra Preta soils do not only exhibit different properties than all adjacent soils in this region (Mann, 2002), but they are also more fertile (Glaser and Birk, 2012). Generally, Terra Preta soils are enriched in soil organic matter (SOM) and do contain higher nutrient levels than adjacent soils (Glaser, 2007; Glaser et al., 2001), rendering them as model soils for sustainable agriculture in the humid tropics (Glaser, 2007; Glaser et al., 2001).

Typically, Terra Preta soils are developed from Ferralsols and Acrisols, but have also been described in a variety of other soil groups including Arenosols, Podzols, Luvisols, Nitisols, and Cambisols (Kern et al., 2003). Naturally occurring Ferralsols, Acrisols, and Arenosols do contain very low amounts of P and basic cations, whereas the Terra Preta soils are usually rich in P, K, Ca, Mg, and also Zn (Falcão et al., 2009; Glaser, 2007; Glaser et al., 2001; Sombroek et al., 2004). Typical concentrations of soil P, for instance, are generally

above 200 mg kg_{soil}⁻¹ of plant-available P, thereby significantly exceeding those of surrounding soils with 5 mg plant-available P kg_{soil}⁻¹ (Falcão et al., 2009). Potential nutrient sources in Terra Preta are: (i) dead plant biomass, (ii) mammal and fish bones, partly as cooking residues (iii) ash, (iv) biochar, and (v) human excrements (Glaser and Birk, 2012). It is widely believed that the lifestyle of the ancient inhabitants has left large amounts of P in Terra Preta sites. Lima et al. (2002) and Schaefer et al. (2004) found evidence that high P and Ca concentrations in some Terra Preta sites were likely derived from bones. Other sources, such as ash (Arroyo-Kalin et al., 2009; Woods and McCann, 2003) and biomass wastes (Lima et al., 2002), could also contribute to the accumulation of P in Terra Preta soils. The determinations of manure-specific steroids (Birk et al., 2010; Birk et al., 2011) and bile acids (Birk et al., 2010; Bull et al., 2002) indicated the enhanced input of faeces from omnivores and especially humans in Terra Preta (Glaser, 2007; Glaser and Birk, 2012; Glaser et al., 2004). Lehmann et al. (2005) demonstrated significant enhancement of total P (from 1,059 to 6,450-13,307 mg kg⁻¹) after long-term (>25 years) poultry manure applications.

Terra Preta soils are usually also less acidic with pH values ranging from 5.2 to 6.4 (Falcão et al., 2009) relative to surrounding Ferralsols or Acrisols, therefore their Al toxicity is reduced and nutrient availability is enhanced. The enrichment with SOM frequently reaches a factor of three (Glaser, 2007), thus contributing to elevated cation exchange capacity (CEC), being between 13 and 25 cmol_c kg⁻¹ (Falcão et al., 2009; Glaser, 2007; Glaser et al., 2001; Sombroek et al., 2004). Parts of this SOM derive from the enrichment in black carbon (BC) (Glaser et al., 2000; Glaser et al., 2004; Lehmann et al., 2003). Residues from incomplete combustion BC may account for up to 35% of the SOM in Terra

96 Preta soils, while adjacent soils only contained 14% of BC in SOM (Glaser et al., 2000).
97 Hence, also BC has been considered as key factor for the long-term fertility and stability
98 of the SOM in Terra Preta (Cornelissen et al., 2005; Glaser et al., 2000; Glaser et al., 2001)
99 and thus also for the maintenance of its elevated CEC (Glaser, 2007; Glaser et al., 2003;
100 Liang et al., 2006). Nevertheless, BC does not contain much P (Hammes et al., 2006), and
101 exchangeable nutrients may also be taken up quickly. Therefore, additional factors must
102 contribute to the sustainable nutrient storage in these soils.

103 A main factor affecting the availability of nutrients in soils and streams, particularly of P,
104 are natural colloids (1-1,000 nm), including nanoparticles or nanocolloids (1-100 nm)
105 (Bollyn et al., 2017; Konrad et al., 2020; Montavo et al., 2015; Stolpe et al., 2013). They
106 may bind large portions of otherwise readily available plant nutrients and organic matter
107 (Carstens et al., 2018; Missong et al., 2018a; Zhang et al., 2017), and they are the key
108 building blocks in the formation of soil micro-aggregates (Krause et al., 2020; Totsche et
109 al., 2018). However, there is little information about the distribution and composition of
110 colloids in Terra Preta soils. Nevertheless, methods to characterize such colloids have
111 become increasingly operational, mostly relying on the fractionation of water-dispersible
112 colloids (WDC, < 1,000 nm in size) into different nanoparticulate (< 100 nm) and fine and
113 medium colloidal materials (< 450 nm) using field-flow fractionation (FFF) (Jiang et al.,
114 2017; Jiang et al., 2015b; Missong et al., 2017; Missong et al., 2018a). Colloids,
115 particularly the smaller WDC < 300 nm, are potentially mobile and can play a more
116 important role for P cycling in soils than coarser particles.

117 The aims of the current study were, therefore, to: i) identify and quantify colloids present
118 in Terra Preta soils and those in adjacent Acrisols, ii) elucidate the role of colloids in Terra

Preta for P binding, and iii) unravel the P species in bulk soil, colloidal fractions and the soil solution. To answer these questions, we sampled surface soils from both Terra Preta and adjacent Acrisol under both forest and arable cropping, respectively, and characterized their WDC composition and P bonding forms, using both FFF and ^{31}P -nuclear magnetic resonance (^{31}P -NMR) spectroscopy, respectively. We hypothesized that colloids in Terra Preta soil do enhance the nutrient retention (including P) due to higher pH and a more abundant organic carbon.

2. Methods and Materials

2.1 Soil sampling and soil properties

Soil samples were collected in the Caldeirão experimental research station from Embrapa Amazônia Ocidental located in Iranduba County in the Brazilian Central Amazon (03°26'S, 60°23'W). The soils were classified according to the World Reference Base for Soil Resources (WRB, 2015). Briefly, our Terra Preta soils were Hortic Anthrosols and the adjacent (ADJ) soils were Haplic Acrisols. Each soil was sampled from a secondary forest site and manioc (*Manihot esculenta*) cultivation site (Table 1). The forested sites were more than 45 years-old in Terra Preta and adjacent soils, while the cultivation sites were ca. 25 years-old in Terra Preta soils and adjacent soils. Soil samples were taken in February 2016, from three randomly chosen points ca. 15 m apart. At each point, the topsoil (0-10 cm) was collected in triplicate being 5 m apart, which were subsequently homogenized to produce a composite soil sample for each main sampling point. The soil characteristics were described previously (Lima et al., 2014; Taketani et al., 2013) and can be summarized as Terra Preta soils exhibiting relatively high pH, CEC as well as Ca, K, Mg, Mn, P, SOC,

and Zn contents when compared to their adjacent soils. In contrast, the adjacent soils showed, however, a lower pH (Table 1) and higher Al and Fe content.

2.2 Sample fractionation and scanning electron microscopy (SEM)

Preceding the scanning electron microscopy, soil texture analysis by sedimentation (results in Table 1) was carried out for all samples twice, with and without destruction of Fe-(hydr)oxides using Na-dithionite. 10 mL aliquots of the clay fractions $<2\ \mu\text{m}$ with and without oxide destructions steps were transferred to 15 mL centrifuge tubes after vigorously mixing the clay suspension by hand. The clay fractions were washed several times with deionized water until free of electrolytes (electrical conductivity $<30\ \mu\text{S cm}^{-1}$). The aqueous sample suspensions were shaken and treated for 2 min in an ultrasonic bath (Bransonic 12, Danbury, USA) before single drops of the suspensions were transferred onto aluminium sample stubs (G301, Plano, Wetzlar, Germany) covered with conductive carbon tabs (G3347, Plano, Wetzlar, Germany) and allowed to dry in a desiccator. A thin gold coating was applied to the samples by ion sputtering. Secondary electron images were recorded on a Zeiss/Leo EM9DSM982 (Oberkochen, Germany) electron microscope at 5 kV. For each sample, (at least) one image per location at magnifications from 1.000 to 50.000x were recorded.

2.3 Analyses of benzene polycarboxylic acids as markers for BC

Hot acid digestion was used to transform BC into benzene polycarboxylic acids (BPCA) (Glaser et al., 1998). For analyses, we followed the revised protocol of Brodowski et al. (Brodowski et al., 2005), keeping strictly the threshold of 5 mg organic carbon

concentration to minimize artefact formation (Kappenberg et al., 2016). Samples were analyzed with a Hewlett Packard 6890 gas chromatograph (Hewlett Packard GmbH, Waldbronn, Germany) equipped with a flame ionization detector and a HP-5 capillary column (30 m x 0.32 mm i.d., 0.25 μ m film thickness, Macherey-Nagel, Düren, Germany; for oven program see Brodowski et al. (Brodowski et al., 2005). All analyses were run in triplicates. The recovery of the internal standard (citric acid) averaged > 85 %. The total amount of BPCAs was corrected for CO₂ loss and insufficient conversion of BC to BPCAs by a factor of 2.27 (Glaser et al., 1998), representing a conservative minimum estimate of BC concentration (Brodowski et al., 2005).

2.4 Extraction and separation of water dispersible colloids

In order to separate differently-sized particles, the soils were firstly dried at the air and sieved to 2 mm to remove stones or large organic particulate plant residual material. Then 10 g of dried soil and 20 mL Milli-Q water were mixed and horizontally shaken at 150 rpm for 6 h. Subsequently, additional 60 mL of Milli-Q water were added and mixed with the soil before the sedimentation. According to the bottle size (i.e. water table height in the bottle), the sedimentation time was calculated for the desired particle size by Stoke's law. For a size fraction of 20–2,000 μ m, the bottle needed to be left for the sedimentation for 10 min. The supernatant ($d < 20 \mu$ m), containing the non-settling phase (aqueous phase + particles < 20 μ m) was transferred to a new bottle, followed by a further sedimentation for 14 h. The supernatant ($d < 2 \mu$ m), containing the non-settling phase (aqueous phase + particles < 2 μ m) was separated by pipette and transferred to centrifugation tubes. From the supernatant ($d < 2 \mu$ m), one half of the liquid was transferred for freeze-drying and the other

half for the separation of the water-dispersible colloid fraction < 300 nm. For the desired WDC < 300 nm the supernatant ($d < 2 \mu\text{m}$) was centrifuged (with the Biofuge, Heraeus) for 10 min at 6,000 g. The centrifugation time was calculated according to Hathaway (1956). Furthermore, dynamic light scattering (DLS) measurement was performed on the separated WDC samples to verify the effectiveness of the size fractionation (Figure S1). The final supernatant containing aqueous phase and WDC ($d < 300$ nm) was the water extractable phase (WEP). Therefore, for specific certain elements, WEP content is the sum of water dispersible colloids-associated content (WDC) and the dissolved phase content (Javidpour et al., 2009) in the aqueous phase.

2.5 Field-flow fractionation

The WDC ($d < 300$ nm) were size separated using asymmetric FFF (AF2000, Postnova Analytics, Landsberg, Germany). The FFF was coupled online to a UV-vis detector (Postnova Analytics), dynamic light scattering detector (DLS; Malvern Instruments), an organic carbon detector (OCD; DOC laboratory Dr. Huber, Germany) and an inductively coupled plasma mass spectrometer (ICP-MS; Agilent 7500, Agilent Technologies, Japan). The content of organic-C, P, Fe, Al, Si, Ca and Mn was determined in the WDC fractions. Further details of the FFF technique and analytical element determination are described elsewhere (Lespes et al., 2015; Schimpf et al., 2000). Details concerning the parameters of the separation method are shown in Table S1 (Missong et al., 2017). Particle size resolution of FFF separation was checked by analyzing latex standards (from Postnova analytics) under the same conditions as the samples, as described by Missong et al. (2018b). The raw data of the ICP-MS measurements were collected in counts per second with the ICP-MS

Mass Hunter Workstation Software (Agilent Technologies, Japan). The raw data of OCD were measured as volts of the detector signal with the AF⁴ analytical software (Postnova, Landsberg, Germany). The peak areas of the separated particle fractions were integrated and converted to the concentration in nmol by means of linear, multipoint calibration. Finally, the results were transformed into the unit $\mu\text{g kg}_{\text{soil}}^{-1}$ considering the water content of the samples and the extracted sample weight. The significant differences between individual groups were tested with P-value in Microsoft Excel® (Microsoft Corporation, Redmond, USA, version 2013).

2.6 ³¹P-nuclear magnetic resonance spectroscopy

To extract a wide range of organic P (P_o) and inorganic P (P_i) compounds, the frequently applied extraction procedure of Cade-Menun and Preston (Cade-Menun and Preston, 1996) was used. Reagents 0.5 M NaOH (Merck, 99.0%) and 0.1 M EDTA (Merck, 99.0%) were mixed in a volume ratio of 1:1. 10 g of the 2 mm sieved soils was extracted with the EDTA+NaOH reagent in a w:v ratio 1:10. The samples were shaken for 16 h on a horizontal shaker at 150 rotations min⁻¹. The extracts were centrifuged at 10,000 g for 30 min. Thereafter the supernatant was decanted and then was freeze-dried. For re-dissolving, 0.400 g of the freeze-dried samples were weighted in a centrifugation tube and 1.5 mL D₂O + 0.015 mL NaOD (30% in D₂O) were added to the samples. The samples were then shaken and vortexed. When the sample was dissolved, the sample was centrifuged for 15 min at 4,000 g. The supernatant was extracted with a pipette and used for the ³¹P-NMR measurement. The ³¹P-NMR measurements were performed on a Bruker 600 Avance NMR-spectrometer operating at 242.95 MHz for ³¹P. The spectra were collected by using

32K data points over an acquisition time of 0.7s. Details of the measurement have been described elsewhere (Missong et al., 2016). The standard for calculation was MDPA (Methylenediposphonic acid, $\text{CH}_2[\text{P}(\text{O})(\text{OH})_2]_2$) at 17.5 ppm. The proportions of different phosphorus species were quantified based on ^{31}P -NMR measurement. The signal of the MDPA area is equivalent to the P concentration in MDPA. The concentrations of P_o and P_i compounds were calculated based on the ratios of their peak areas to the standard peak area.

3. Results

3.1 Black carbon and soil-particle morphology

The soil organic carbon concentration (0-10 cm) was predominantly related to land use, with the values in forests exceeding those of the manioc sites by at least 10 g C kg^{-1} , irrespective of soil group. However, elevated contributions of BC to SOC, ranging from ca. 19-26%, were found consistently in the Terra Preta soils (Figure 1), thus supporting the assumption that they were likely of anthropogenic origin. This went along with slightly lower ratios of penta- to hexacarboxylated benzoic acid markers (b5ca/b6ca).

SEM images were determined on $<2 \mu\text{m}$ particles of the clay fractions to obtain insight on their morphology, both with and without destruction of iron-(hydr)oxides. The clay contents determined after the destruction of iron-(hydr)oxides were about 5% smaller than in samples that were not treated with Na-dithionite, because also iron-(hydr)oxides are $< 2 \mu\text{m}$ in size. Particles on SEM images from samples with iron oxides destroyed in Figure 2 e-h appeared sharper as presumably they were not covered by an amorphous iron oxide-phase. Overall, Figure 2 showed that the samples consisted of quite a heterogeneous mixture of differently shaped particles. Beside a multitude of small platelets, as well as of

clear (pseudo)hexagonal larger particles typical for kaolinites, a thin crack-forming “gel-”like film was “covering” particles in the oxide-containing samples, this was especially pronounced at the forest sites (Figure 2 a-b). In addition, some half-moon-shaped porous structures were present, most likely consisting of glassy/ ash material together with a few larger structures. The latter had biogenic features but were of an unknown origin (Figure 2e).

3.2 Size distribution and elemental content of water-dispersible colloids

The FFF fractograms based on the online detection by UV, OCD and ICP-MS give information about the colloidal size and composition of the soil WDC-extracts (< 300 nm). Three WDC size fractions were identified for the soils at the four sites (Figure 3) according to the calibration curve as described by Missong et al. (2018b). The first eluting peak presented the pure nanocolloidal fraction (NC; 0.6 - 30 nm) according to the independent analysis of latex standards by DLS (Missong et al., 2018b). The second peak (30 - 240 nm) corresponded to fine colloids fraction (FC). Note, this fraction contained also 30-100 nm nanoparticles but it was dominated by 100-240 nm sized fine colloids (Figure 3 and S1). Finally, we classified the third peak (240 - 300 nm) as the medium-sized colloids fraction (MC). The relative proportions of three WDC size fractions (NC, FC and MC) differed between Terra Preta soils and adjacent soils (Figure 3). All three size fractions contained SOC, though with lower absolute concentrations in the adjacent Acrisols (Figure 3a, Table 2). The elemental concentrations associated to WDC highlighted that besides OC, Al, Si, and Fe, also elements present in smaller concentrations like Ca, Mg, Mn, and Zn, were larger in the Terra Preta soils than in the respective fractions of the adjacent Acrisols (Table

2). When looking at individual size fractions, significantly larger concentrations of Al and Si were detected bound to the NC fraction in the adjacent Acrisols than to those in the Terra Preta (Table 2). Terra Preta soils, in turn, had the highest concentration of FC- and MC-associated Si, Al, Fe and Ca (Table 2). Results for Zn were ambiguous. Noteworthy, for all other elements except P, the ratio of element concentrations of WDC to WEP was always larger for the Terra Preta soils than for the adjacent ones (Table 3). Furthermore, the detected concentrations of P were higher in both WDC and WEP fractions in the Terra Preta, however, the ratio WDC/WEP for P was lower in Terra Preta.

3.3 Phosphorus in bulk soils and water dispersible colloids

Phosphorus (P) deserves particular attention because P limitation is widespread in terrestrial tropical ecosystems, but is perceived to be less pronounced in Terra Preta soils (Table 2) relative to the more common Acrisols. Larger portions of MC-carrying P were detected in Terra Preta soils than in the adjacent Acrisols (Table 2), which is in line with the overall size distribution of WDC in the four soils (Figure 3 and S2). Similar to the other elements, the NC fraction was the main carrier of WDC-associated P in the Acrisols. However, the P contents carried by NC in Terra Preta soils and adjacent soils were not significantly different from each other (Table 2), in contrast to the concentrations of P bound to FC (Figure 3 and S2).

The P species composition detected by ^{31}P -NMR spectroscopy was dominated by orthophosphate (5.89 to 5.68 ppm; orthophosphate was present as H_2PO_4^- in the 3.8-6.0 pH range of the soils studied) in bulk soils and in 30-300 nm sized colloids, followed by orthophosphate monoesters (3 to 5.8 ppm) and orthophosphate diesters (-1.0 to 2.5 ppm)

(Figure 4 and S3) and in line with shift differences described in literature (Cade-Menun, 2015; Turner et al., 2003). The aqueous phase including colloids < 30 nm in Terra Preta soils and adjacent forest soils only contained orthophosphate, whereas in the aqueous phase including colloids < 30 nm of adjacent manioc soils no P was detected by ³¹P-NMR spectroscopy (Figure 4 and S3). Overall in Terra Preta soils, the proportion of orthophosphate rose from 71% in bulk soils to 83%~86% in 30-300 nm sized colloids, and to 100% in the aqueous phase including colloids < 30 nm. The proportion of orthophosphate monoesters in Terra Preta soils diminished from 23%~24% in bulk soils to 11%~13% in 30-300 nm sized colloids. All four bulk soils did also contain some orthophosphate diesters (including RNA hydrolysis products signed as signal “n” in Figure S3), the proportions of which being generally largest in the adjacent forest soil, and were generally larger in the Acrisols than in the corresponding Terra Preta soils (Figure 4). The adjacent soils also contained phosphonates (only at around 20 ppm in our research), not found in the Terra Preta soils (Figure 4 and S3). Pyrophosphate (-4 to -4.6 ppm) was present in small amount in all bulk soils, but again, adjacent soils (0.8%~1.4%) contained higher percentages of pyrophosphate than Terra Preta soils (0.1%) (Figure 4). In addition, phospholipids (including α-glycerophosphate at 4.68 to 4.54 ppm and β- glycerophosphate at 4.48 to 4.24 ppm) were detected in all bulk soils, accounting for 4%~6% in adjacent Acrisols compared to 2% in Terra Preta soils (Figure 4).

4. Discussion

4.1 Black carbon

The Terra Preta soils showed elevated BC contents, as typical for this soil genesis with large inputs of fire remains from cooking remains and kitchen fire places (Atkinson et al., 2010; Glaser et al., 2004). The latter usually exhibit higher fire temperatures than common vegetation burning events. Higher temperatures usually result in higher degree of aromatic condensation and thus lower ratios of penta- to hexacarboxylic benzoic acids (b5ca/b6ca) (Wolf et al., 2013). These ratios were indeed slightly lower in the Terra Preta soils (Figure 1), thus supporting the idea of anthropogenic inputs of BC remains. It should be noted that high temperature fires do not only introduce BC but also ashes, thereby also contributing to essential nutrients like P and basic cations, and possibly even carbonates, which increase the soil pH and therewith promote colloid formation as outlined below.

4.2 Water-dispersible colloids in Terra Preta and adjacent soils

The presence of WDC in Terra Preta soils and adjacent forest soil went along with an enrichment of SOC, while at the adjacent manioc site the colloidal SOC concentration was low (Figure 3 and Table 2). On the one hand, these data reflect effects of management on SOC storage. Deforestation resulted in significant SOC losses (Davari et al., 2020; Khormali et al., 2009), and at the manioc site without natural SOC supply, the SOC-containing NC fraction was absent. In contrast, the clear presence of NC associated SOC in the forest topsoils might be related to the natural formation of SOC containing nanoparticles after the degradation of litter, as also found for other forest sites (Missong et

al, 2017). On the other hand, the data point to soil-group specific effects of soil aggregation and related organic matter storage processes. Comparing the elemental compositions to that found in other ecosystems (Gottselig et al., 2017; Jiang et al., 2015a; Missong et al., 2018a), it is reasonable to suspect that the dominant WDC components were organic matter, clay minerals and Fe-, Al- (hydr)oxides such as goethite and hematite (Chia et al., 2012; da Costa and Kern, 1999; Lima et al., 2002), of which clay mineral platelets have been confirmed by morphological observation (Figure 2).

The stoichiometry ratio between Al:Si in the WDC was 1:1 (Table 2), as characteristic e.g. for kaolinite, the typical phyllosilicate in Acrisols and as also described by da Costa et al. (2003) to be the most abundant phyllosilicate in Amazonian dark earth. Additionally, Ruivo et al. (2004) and Glaser et al. (2004) have confirmed the predominance of kaolinite in the clay fraction in both Terra Preta soils and their surrounding soils. Also our SEM images indicate this by the observation of (pseudo)hexagonal structures typical for kaolinite (Figure 2).

We found that WDC in Terra Preta soils contained larger particles consisting of minerals and organic matter. We attribute this to the formation of organo-mineral associations by the increasing presence of bivalent cations like Ca^{2+} and Mg^{2+} (see Table 1) from ash and bones. Ca^{2+} and Mg^{2+} can facilitate cation bridging and thus association of small building blocks to fine- and medium-sized colloids. The water extractable Ca^{2+} and Mg^{2+} concentrations (soluble Ca and Mg) were 10-30 times higher in Terra Preta soils than in adjacent Acrisols. The cation bridging effect with SOM increases with increasing pH, due to increasing deprotonation of, e.g., carboxylic groups bound to mineral matter (Chorover et al., 2004; Marschner et al., 2008; Saidy et al., 2012; von Lutzow et al., 2006).

368 Additionally, due to their positively charged surfaces, Fe oxides promote the formation of
369 colloidal associations with kaolinite and organic matter (Saidy et al., 2013; Tombácz et al.,
370 2004). The elevated pH values in the Terra Preta soil likely promoted reactions of SOM
371 with iron oxides in addition to the sorption of basic cations. The significantly larger SOM
372 contents in Terra Preta FC and MC than those in adjacent Acrisols lead to the assumption
373 that the more nutrients can be retained by organic-mineral associations in Terra Preta soils,
374 and can thus reside in soil for periods of time. Any attempt to reconstruct Terra Preta WDC
375 must therefore assure that elevated pH values with related inputs of basic cations are
376 maintained, not only to reduce Al toxicity, but also to promote and sustain the respective
377 colloidal organic-mineral forming processes.

378 Water-extractable phase (WEP) represents a mobile soil fraction, which includes both
379 colloidal (WDC) and truly dissolved phases. The truly dissolved phases are easily taken in
380 by plants and micro-organisms, but still they usually represent a significant source of soil
381 nutrient losses (Hussain et al., 2020; Perakis and Hedin, 2002; Walton et al., 2020).
382 However, in colloids the nutrients are retained and present as exchangeable (adsorbed onto
383 colloids) or structural (tightly bound in colloids) components (Missong et al., 2018a). The
384 higher ratios of WDC to WEP suggested an enhanced retention effect of Terra Preta on
385 most nutrients, except P. Terra Preta soils did contain more of the larger sized colloid
386 fractions with a lower mobility than nanoparticles when compared to adjacent soils.

388 **4.3 Phosphorus in bulk soils and colloids**

389 The total P concentrations of Terra Preta soils were notably higher than adjacent soils
390 (Table 1). Glaser (1999) reported total P values of 980-2,170 mg kg⁻¹ for five different

Anthrosols from central Amazonia. Lehmann et al. (2004) also reported the total P contents varying from 193 to 3,097 mg kg⁻¹, which were far above the ones (40-100 mg kg⁻¹) from acid upland soils of central Amazonia. The dominance of inorganic P forms (Figure 4) was opposite to other forest soils (Guggenberger et al., 1996; McDowell et al., 2007; Missong et al., 2016; Turner and Engelbrecht, 2011) or forest drainage (Kaiser et al., 2003; McDowell and Stewart, 2005) in temperate climates, in which P_o usually accounted for a half or a larger portion of all P. We do not attribute this finding to the different mineralogy of tropical soils relative to those studied so far in temperate climates, but rather to the enhanced inputs of P into the topsoils, via, e.g., manure- and other excrements (Lehmann et al., 2005), and fire residues (Turrión et al., 2010).

The high P content associated to the colloidal fractions correlates with Fe and Ca contents rather than with those of SOC (Table 2). The fine and medium-sized colloids in Terra Preta soils may occlude P and thus contribute to its prolonged P storage capacity (Glaser, 1999; Lehmann et al., 2004). In the adjacent Acrisols with low soil pH, the binding of remaining P to positively charged Fe-oxide surfaces may limit its availability (Haygarth et al., 1997). P in the Terra Preta soils appears largely to be occluded within the larger-sized colloidal organic-mineral associations, where it might be less strongly fixed by oxides due to the higher pH values (Gustafsson et al., 2012; Zhang et al., 2019), and thus potentially more available for plants and microorganisms than in the adjacent Acrisols. The elevated content of WDC-associated Ca in Terra Preta soils (Table 2) may contribute to the retention of P, likely via the effect of Ca²⁺ on the formation of organo-mineral associations and bridging of anionic P like orthophosphate (SOM-Ca-P bridges; Yan et al., 2016) rather than by direct precipitation reactions as apatite-like minerals, which should be more or less dissolved at

414 ambient pH. Overall, dissolved and colloidal phosphorus in aqueous phase, e.g.
415 orthophosphate and monoesters, may contribute to their bioavailability in soils (Missong
416 et al., 2016). Therefore, the fertility of Terra Preta soils was enhanced due to elevated P
417 contents in colloids and aqueous phase combined with higher portions of orthophosphate
418 and monoesters.

420 **5. Conclusion**

421 Field flow fractionation results showed that water-dispersible < 300 nm colloids in Terra
422 Preta soils contained a significant proportion of organo-mineral associations in the size
423 range 30-300 nm, whereas, in contrast, water-dispersible < 30 nm nanoparticles were
424 dominant in the adjacent Acrisols. The lower soil pH values in the Acrisol facilitated
425 nanoparticle formation between kaolinite-like clay minerals, Fe-(hydr)oxides and OM in
426 the acid Acrisols. Vice versa, elevated pH values and elevated concentrations of bivalent
427 cations in the Terra Preta soils, initiated from increased inputs from ash and bones, led to
428 the formation of larger sized colloidal organo-mineral associations with larger portions of
429 OM and resulted in an enhanced retention of phosphorus. The well-known
430 recommendation that soil acidification in these tropical soils should be prevented or
431 reversed does therefore not only apply to Acrisols, but is also at least as crucial for colloid
432 formation processes and related fertility in the Terra Preta soils. Altogether, the interplay
433 of ash-initiated pH rise, subsequent reduced aluminum toxicity, elevated concentrations of
434 dissolved bivalent cations from ash and bones and resulting elevated biomass input thus
435 contributed to improved soil fertility in Terra Preta soils.

Acknowledgements

Qian Zhang would like to thank the China Scholarship Council (No. 201608420100) for supporting her study at Forschungszentrum Jülich GmbH and RWTH Aachen University.

The authors would like to thank Dr. Volker Nischwitz, from Central Institute for Engineering, Electronics and Analytics, Analytics (ZEA-3), Forschungszentrum Jülich GmbH, for the support with the ICP-MS measurements. We thank Dr. Liming Wang, from Institute of Bio- and Geosciences, Agrosphere (IBG-3), Forschungszentrum Jülich GmbH, for his support with ^{31}P -NMR analysis. We thank Dr. Martin Hardt and co-workers, from the Microscopy and Imaging Center at the Biomedical Research Center Seltersberg, University of Giessen, for their support with scanning electron microscopy, and I. Wieland (Bonn) for help with BC analyses. We thank Embrapa (Brazilian Agricultural Research Corporation) for its support in this research.

449 Table 1. Soil chemical properties of terra preta de índico soils (TPI) and their adjacent soils (ADJ) under
 450 secondary forest (Forest) and Manioc plantation (Manioc). Mean values soil texture analysis: Standard
 451 texture analysis and texture including the oxide destruction step. Concentrations of P, Fe, Al, Zn, Mn, K,
 452 Mg and Ca in mg dm^{-3} and $\text{cmol}_c \text{ dm}^{-3}$ are soil extractable elements.

Soil properties	TPI-Forest	TPI-Manioc	ADJ-Forest	ADJ-Manioc
Soil type and use	Terra preta de índico forest	Terra preta de índico manioc plantation	Adjacent forest	Adjacent manioc plantation
Classification	Hortic Anthrosol	Hortic Anthrosol	Haplic Acrisol	Haplic Acrisol
% sand	64	67	73	65
% silt	9	8	3	4
% clay	27	25	24	31
% sand (incl. oxides)	59	63	68	59
% silt (incl. oxides)	8	7	4	4
% clay (incl. oxides)	33	30	28	36
pH (0.01 M CaCl_2)	4.8	4.5	3.6	3.7
pH (water) [★] °	5.1-6.1	5.0-5.6	3.7-3.9	3.7-4.2
Organic carbon (g kg^{-1}) [★] °	29.0-35.7	11.8-14.5	9.8-13.6	10.6-11.1
Organic matter (g kg^{-1}) [°]	44.1-52.9	44.9-46.2	29.3-35.0	27.0-28.6
Total P (mg kg^{-1})	1223-1425	1045-1358	352-385	265-270
P (mg dm^{-3}) [★] °	43.7-88.6	68.8-249.6	3.1-7.2	0.8-4.6
Fe (mg dm^{-3}) [★] °	14-28	19-55	249-366	150-286
Al ($\text{cmol}_c \text{ dm}^{-3}$) [★] °	0.01-0.05	0.01-0.29	1.5-1.9	1.3-1.5
Zn (mg dm^{-3}) [★] °	6.3-12.3	2.0-13.4	0.3-0.5	0.4-1.8
Mn (mg dm^{-3}) [★] °	40-61	19-39	1.1-3.0	0.9-2.1
K (mg dm^{-3}) [★] °	26.6-49.7	13.8-22.3	14.0-24.4	14.2-24.6
Mg ($\text{cmol}_c \text{ dm}^{-3}$) [★] °	0.7-1.6	0.8-1.4	0.05-0.13	0.05-0.16
Ca ($\text{cmol}_c \text{ dm}^{-3}$) [★] °	2.3-4.5	3.3-4.4	0.05-0.33	0.09-0.38

453 ★: Lima, A.B., Muniz, A.W., Dumont, M.G., 2014. Activity and abundance of methane-oxidizing bacteria in secondary forest and manioc
 454 plantations of Amazonian Dark Earth and their adjacent soils. *Frontiers in microbiology* 5, 550.

455 ©: Taketani, R.G., Lima, A.B., da Conceição Jesus, E., Teixeira, W.G., Tiedje, J.M., Tsai, S.M., 2013. Bacterial community composition
456 of anthropogenic biochar and Amazonian anthrosols assessed by 16S rRNA gene 454 pyrosequencing. *Antonie van Leeuwenhoek* 104(2),
457 233-242.

Table 2. Concentrations of elements in WDC (<300nm) of four soils ($\mu\text{g kg}_{\text{soil}}^{-1}$). The concentrations of each element in NC, FC and MC fractions were calculated by integrating the FFF-ICP-MS-OCD patterns. TPI= terra preta de índico soil; ADJ=adjacent soil. Nanocolloids fraction (NC) is from 0.6nm to 30nm; Fine colloids fraction (FC) is from 30nm to 240nm; Medium-sized colloids fraction (MC) is from 240nm to 300nm. Mean values and standard deviations for three replicates in each group. ^{a b c d}=significant differences ($p<0.05$) between four groups (sites).

Soil type	Fraction	SOC ($\mu\text{g kg}_{\text{soil}}^{-1}$)	Mg	Al	Si	P	Ca	Mn	Fe	Zn
Forest	all	20.0 \pm 1.0 ^a	78 \pm 8 ^a	3386 \pm 1586 ^{ab}	3715 \pm 1777 ^a	94 \pm 36 ^a	481 \pm 64 ^a	9.9 \pm 2.7 ^a	2130 \pm 874 ^a	6.5 \pm 1.7 ^a
	TPI	5.7 \pm 0.8 ^a	4 \pm 1 ^a	41 \pm 9 ^c	44 \pm 11 ^c	7 \pm 2 ^a	52 \pm 9 ^a	0.4 \pm 0.1 ^a	19 \pm 5 ^b	0.9 \pm 0.2 ^a
	FC	7.0 \pm 0.2 ^a	32 \pm 2 ^a	440 \pm 306 ^{ab}	448 \pm 334 ^{ab}	17 \pm 10 ^a	220 \pm 19 ^a	2.5 \pm 0.6 ^a	479 \pm 276 ^a	2.0 \pm 0.5 ^a
	MC	7.2 \pm 0.5 ^a	42 \pm 6 ^a	2904 \pm 1271 ^a	3223 \pm 1433 ^a	70 \pm 27 ^a	208 \pm 55 ^a	6.9 \pm 2.1 ^a	1632 \pm 594 ^a	3.6 \pm 1.2 ^a
Forest	all	12.3 \pm 3.9 ^a	20 \pm 10 ^b	2509 \pm 1269 ^{ab}	2290 \pm 1099 ^a	36 \pm 13 ^a	98 \pm 69 ^c	2.4 \pm 0.8 ^b	1970 \pm 1092 ^a	5.3 \pm 2.6 ^a
	ADJ	4.4 \pm 2.0 ^a	17 \pm 0.4 ^b	1861 \pm 1075 ^a	1654 \pm 937 ^a	28 \pm 12 ^a	42 \pm 5 ^c	1.1 \pm 0.2 ^b	1542 \pm 949 ^a	2.6 \pm 0.1 ^a
	FC	4.7 \pm 1.5 ^{ab}	5 \pm 6 ^b	453 \pm 148 ^b	420 \pm 128 ^b	0 \pm 4 ^a	30 \pm 37 ^b	0.7 \pm 0.6 ^b	308 \pm 116 ^b	1.7 \pm 1.6 ^a
	MC	3.2 \pm 0.5 ^b	8 \pm 5 ^b	194 \pm 55 ^b	216 \pm 49 ^b	8 \pm 1 ^b	25 \pm 27 ^b	0.6 \pm 0.4 ^b	119 \pm 29 ^b	1.1 \pm 1.0 ^a
Manioc	all	19.0 \pm 5.8 ^a	79 \pm 11 ^a	7309 \pm 3989 ^a	7602 \pm 3908 ^a	141 \pm 89 ^a	321 \pm 73 ^b	14.2 \pm 6.3 ^a	5373 \pm 3073 ^a	10.0 \pm 4.9 ^a
	TPI	4.9 \pm 1.8 ^a	4 \pm 0.2 ^a	57 \pm 25 ^b	64 \pm 21 ^b	13 \pm 7 ^a	43 \pm 6 ^b	0.5 \pm 0.1 ^a	57 \pm 32 ^{ab}	0.9 \pm 0.1 ^a
	FC	6.4 \pm 2.0 ^a	34 \pm 7 ^a	2995 \pm 2251 ^a	3036 \pm 2223 ^a	59 \pm 52 ^a	150 \pm 43 ^a	5.7 \pm 3.5 ^a	2723 \pm 2009 ^a	4.3 \pm 2.7 ^a
	MC	7.8 \pm 2.8 ^{ab}	41 \pm 4 ^a	4258 \pm 1718 ^a	4502 \pm 1674 ^a	69 \pm 30 ^a	128 \pm 24 ^a	8.0 \pm 2.7 ^a	2593 \pm 1044 ^a	4.8 \pm 2.2 ^a
Manioc	all	3.9 \pm 0.1 ^b	7 \pm 1 ^b	1254 \pm 765 ^b	1264 \pm 731 ^a	22 \pm 15 ^a	36 \pm 13 ^c	0.6 \pm 0.1 ^c	880 \pm 559 ^a	1.8 \pm 0.3 ^b
	ADJ	0.5 \pm 0.1 ^b	4 \pm 0.4 ^b	803 \pm 557 ^{ab}	794 \pm 550 ^{ab}	12 \pm 3 ^a	19 \pm 2 ^d	0.4 \pm 0.2 ^c	604 \pm 430 ^a	1.1 \pm 0.1 ^b
	FC	1.6 \pm 0.2 ^b	1 \pm 0.3 ^b	349 \pm 178 ^b	335 \pm 165 ^c	0 \pm 6 ^a	8 \pm 2 ^b	0.1 \pm 0.1 ^b	215 \pm 110 ^c	0.4 \pm 0.1 ^b
	MC	1.7 \pm 0.2 ^c	2 \pm 2 ^c	102 \pm 34 ^b	136 \pm 19 ^c	10 \pm 11 ^b	9 \pm 10 ^b	0.1 \pm 0.1 ^b	61 \pm 21 ^b	0.3 \pm 0.3 ^b

Table 3. Element concentration ($\mu\text{g L}^{-1}$) in water extractable phase (WEP, measured by ICP-MS and OCD) and water dispersible colloids (WDC, integrated FFF-ICP-MS-OCD patterns calculated by molar mass of respective element) as well as the concentration ratio. TPI= terra preta de índico soil; ADJ=adjacent soil. Mean values and standard deviations for three replicates in each group. a b c = significant differences ($p < 0.05$) between four groups (sites).

Soil type		SOC	Mg	Al	Si	P	Ca	Mn	Fe	Zn
TPI-Forest	WEP	8864 \pm 736 ^a	2117 \pm 458 ^a	962 \pm 161 ^a	1940 \pm 73 ^a	693 \pm 96 ^a	10717 \pm 3031 ^a	76 \pm 65 ^b	610 \pm 136 ^b	8 \pm 3 ^b
	WDC	2516 \pm 95 ^a	9.9 \pm 1.0 ^a	428 \pm 197 ^a	469 \pm 221 ^a	12 \pm 5 ^b	61 \pm 8 ^a	1.25 \pm 0.33 ^a	269 \pm 109 ^a	0.8 \pm 0.2 ^a
	WDC/WEP	29% \pm 2% ^a	0.5% \pm 0.1% ^{ab}	47% \pm 26% ^a	24% \pm 11% ^{ab}	2% \pm 1% ^c	0.6% \pm 0.2% ^{ab}	4.9% \pm 5.0% ^a	46% \pm 21% ^a	12% \pm 6% ^a
ADJ-Forest	WEP	10620 \pm 4070 ^a	1463 \pm 503 ^{ab}	1933 \pm 406 ^a	1940 \pm 340 ^a	76 \pm 19 ^b	5813 \pm 2201 ^a	214 \pm 29 ^a	1153 \pm 250 ^{ab}	18 \pm 1 ^a
	WDC	1594 \pm 504 ^a	2.6 \pm 1.3 ^b	325 \pm 164 ^a	297 \pm 142 ^a	4 \pm 2 ^a	13 \pm 9 ^c	0.31 \pm 0.11 ^b	256 \pm 142 ^a	0.7 \pm 0.3 ^a
	WDC/WEP	16% \pm 2% ^c	0.2% \pm 0.2% ^b	16% \pm 6% ^{ab}	14% \pm 6% ^b	5% \pm 1% ^b	0.4% \pm 0.4% ^{ab}	0.2% \pm 0.1% ^b	20% \pm 9% ^{ab}	4% \pm 2% ^{ab}
TPI-Manioc	WEP	8762 \pm 2448 ^a	1625 \pm 739 ^{ab}	1703 \pm 634 ^a	2337 \pm 613 ^a	429 \pm 177 ^a	4220 \pm 1825 ^a	76 \pm 58 ^{ab}	996 \pm 370 ^{ab}	19 \pm 6 ^{ab}
	WDC	2413 \pm 738 ^a	10.3 \pm 1.7 ^a	961 \pm 547 ^a	998 \pm 534 ^a	18 \pm 12 ^{ab}	42 \pm 11 ^b	1.86 \pm 0.86 ^a	706 \pm 418 ^a	1.3 \pm 0.7 ^a
	WDC/WEP	27% \pm 1% ^a	0.8% \pm 0.4% ^a	54% \pm 23% ^a	40% \pm 16% ^a	4% \pm 2% ^c	1.2% \pm 0.6% ^a	4.9% \pm 3.5% ^a	66% \pm 30% ^a	9% \pm 7% ^{ab}
ADJ-Manioc	WEP	2192 \pm 43 ^b	946 \pm 175 ^b	1490 \pm 115 ^a	2037 \pm 47 ^a	21 \pm 1 ^c	1720 \pm 329 ^a	29 \pm 5 ^b	1097 \pm 87 ^a	29 \pm 9 ^{ab}
	WDC	499 \pm 16 ^b	1.0 \pm 0.1 ^b	162 \pm 98 ^a	163 \pm 94 ^a	3 \pm 2 ^a	5 \pm 2 ^c	0.07 \pm 0.02 ^c	113 \pm 71 ^a	0.2 \pm 0.04 ^a
	WDC/WEP	23% \pm 1% ^b	0.1% \pm 0.01% ^b	11% \pm 7% ^b	8% \pm 5% ^b	13% \pm 9% ^a	0.3% \pm 0.04% ^b	0.3% \pm 0.1% ^b	11% \pm 7% ^b	1% \pm 1% ^b

Figure 1. Organic carbon (C_{org}) and black carbon (BC) contents on terra preta soils (TPI) and adjacent Acrisols (ADJ) under forest and manioc management

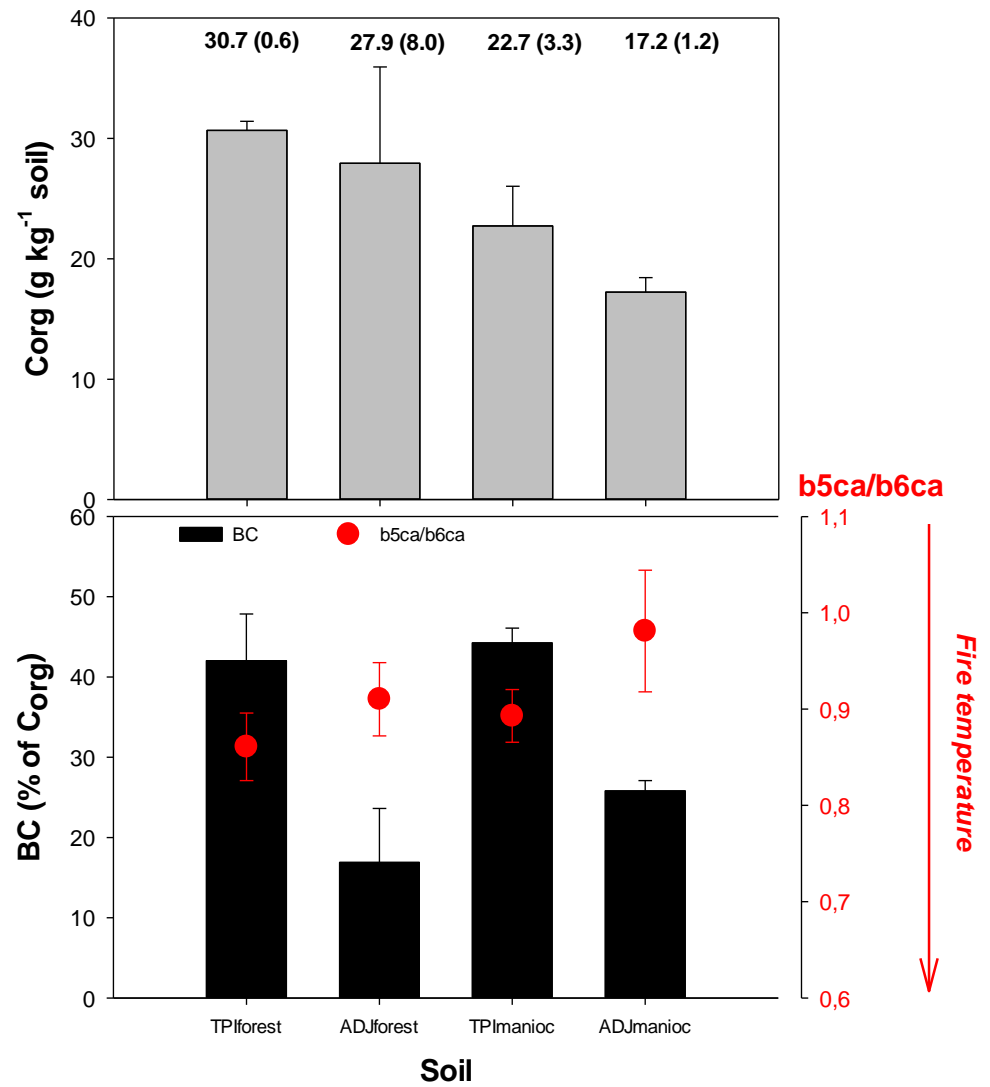


Figure 2. Scanning electron microscope (SEM) images of WDC in 4 soils at 10000-fold magnification. Two groups of samples for SEM: I < 2 μ m, carbonate and organic matter destroyed; II < 2 μ m, carbonate, organic matter and oxides destroyed. ADJ = adjacent Acrisol; TPI = Terra Preta do indio soil.

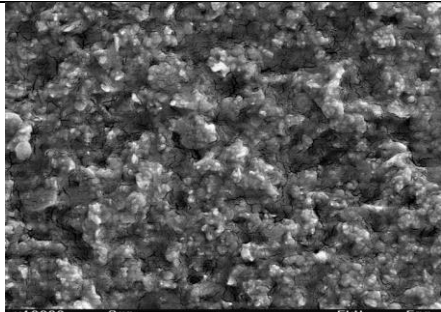
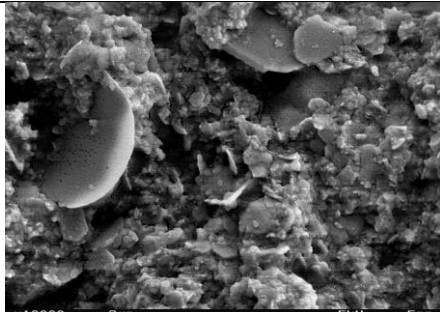
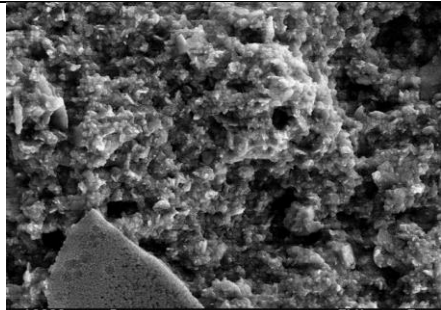
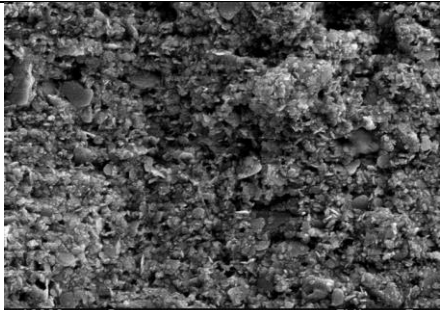
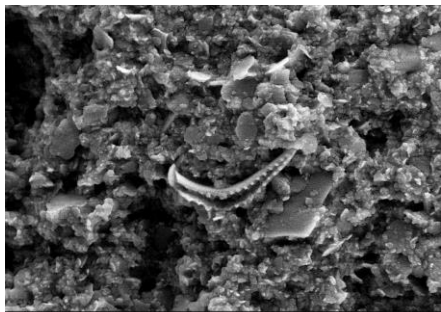
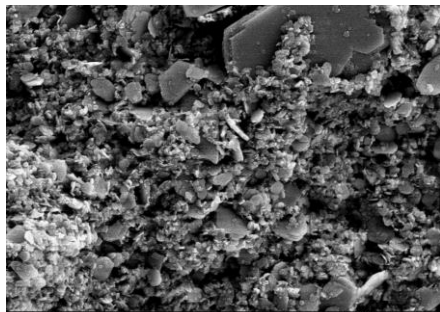
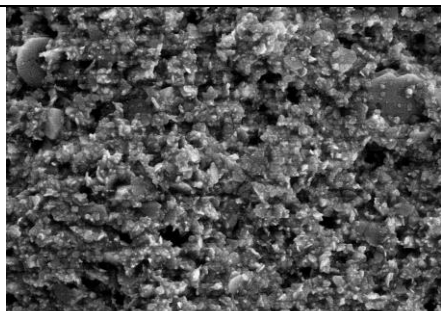
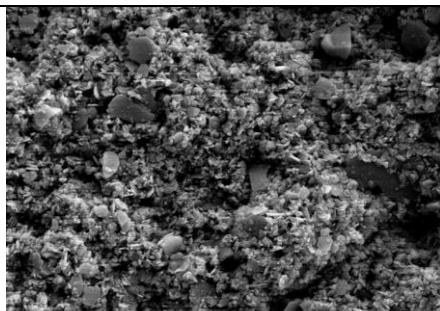
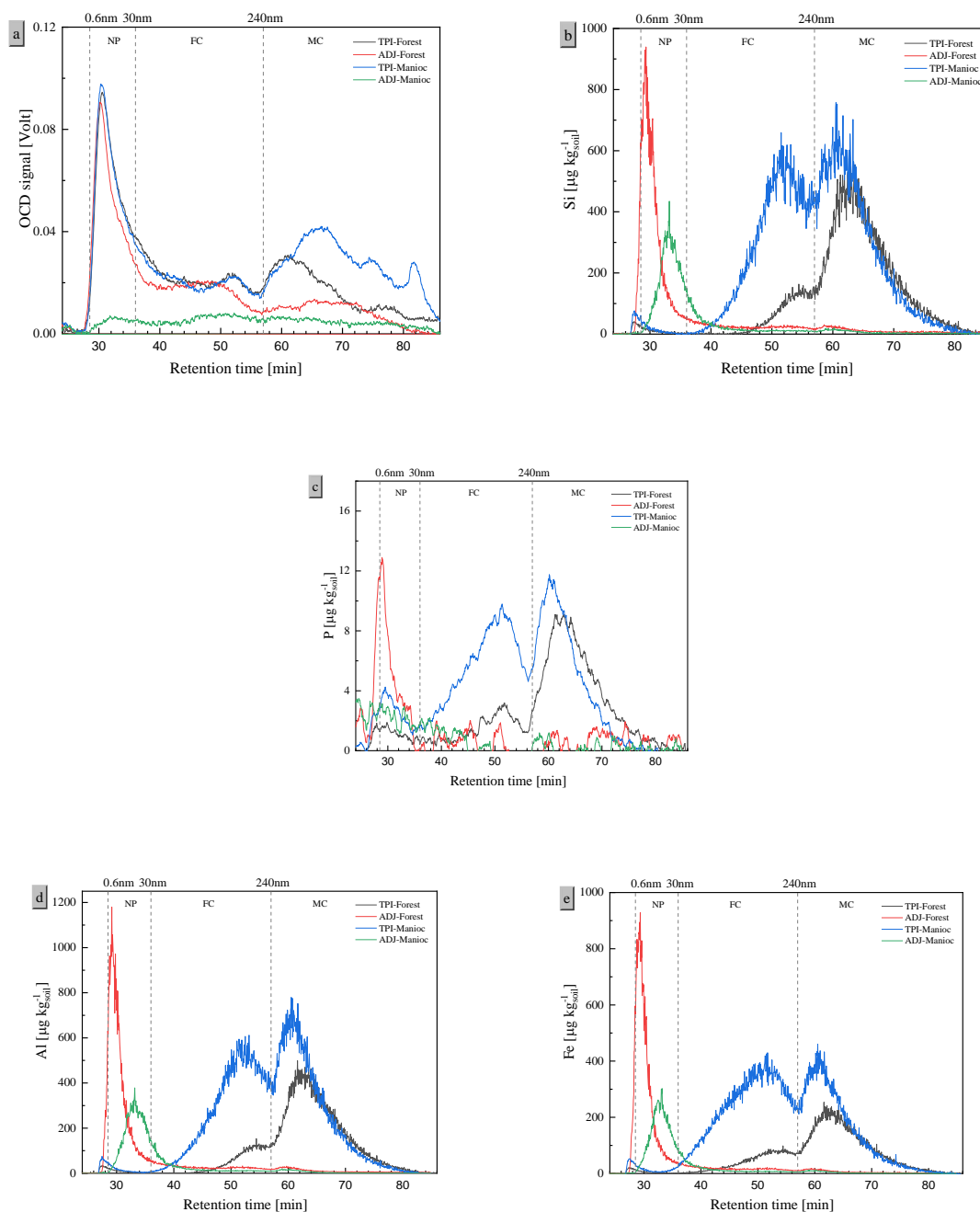
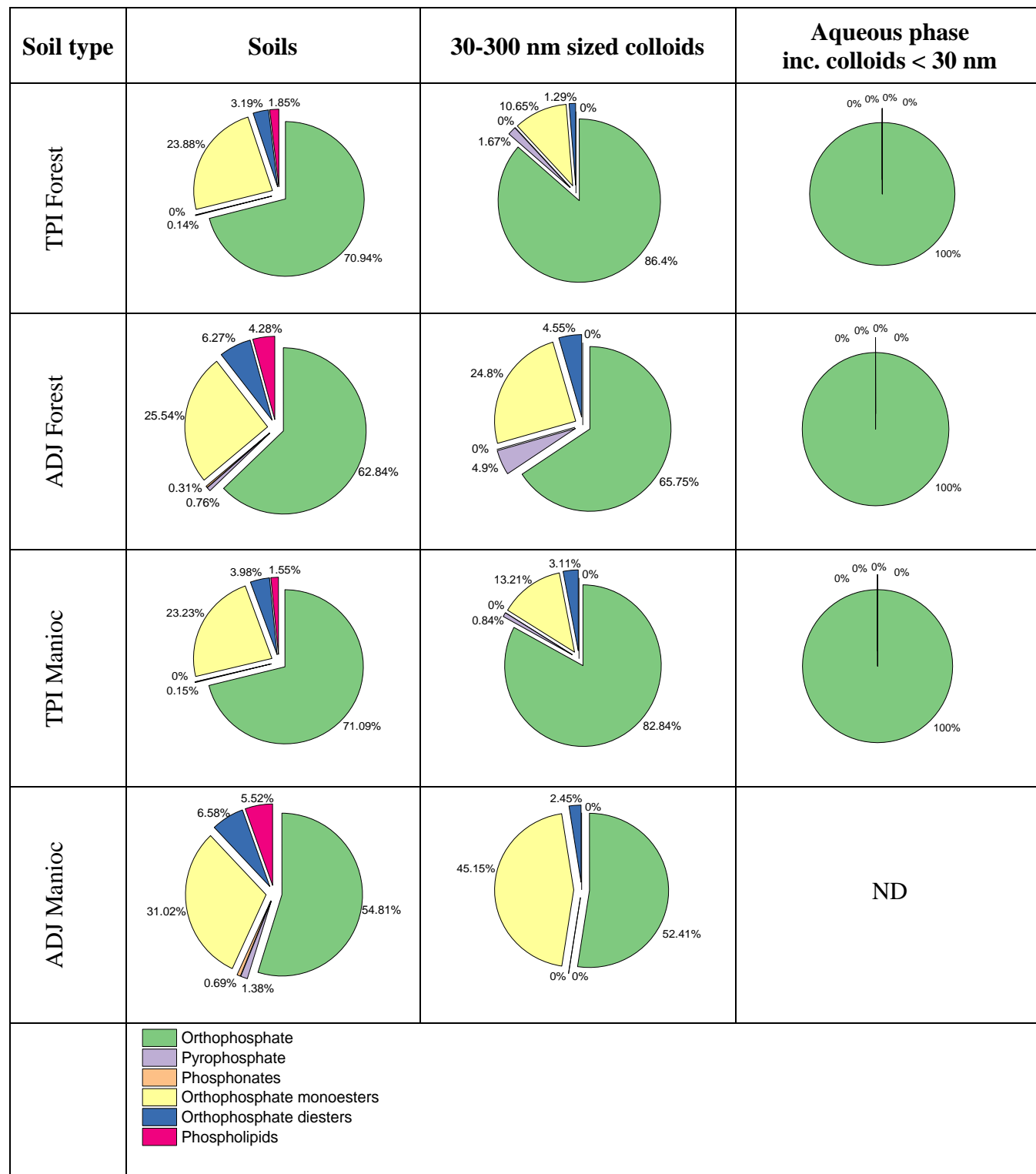
	Carbonate and organic matter destroyed	Carbonate, organic matter and oxides destroyed
TPI Forest	 <p>a)</p>	 <p>e)</p>
ADJ Forest	 <p>b)</p>	 <p>f)</p>
TPI Manioc	 <p>c)</p>	 <p>g)</p>
ADJ Manioc	 <p>d)</p>	 <p>h)</p>

Figure 3. WDC elemental FFF-OCD-ICP-MS fractograms for the 4 soil sites. The y-axis scales in b), c), d), e) were adapted to the actual detected concentration levels (given in μg per kilogram dry soil). The elution time scale was converted in particle size in the x-axis. TPI= terra preta de índico soil; ADJ=adjacent soil. Nanocolloids fraction (NC) is from 0.6nm to 30nm; Fine colloids fraction (FC) is from 30nm to 240nm; Medium-sized colloids fraction (MC) is from 240nm to 300nm.



Note: The highest measurement signals of element were selected from every three replicates. The data of other replicates can be seen from in Figure S2.

Figure 4. Proportions of phosphorus species in bulk soils, 30-300 nm sized colloids and aqueous phase including colloids < 30 nm in four soils. The phosphorus species data were based on ^{31}P -NMR measurement. Each proportion is the mean value of three replicates in the group. TPI= terra preta de índico soil; ADJ=adjacent soil.



References

- Arroyo-Kalin, M., Neves, E.G., Woods, W.I., 2009. Anthropogenic dark earths of the Central Amazon region: remarks on their evolution and polygenetic composition, Amazonian dark earths: Wim Sombroek's vision. Springer, pp. 99-125.
- Atkinson, C.J., Fitzgerald, J.D., Hipps, N.A., 2010. Potential mechanisms for achieving agricultural benefits from biochar application to temperate soils: a review. *Plant Soil* 337(1-2), 1-18.
- Birk, J., Teixeira, W., Neves, E., Glaser, B., 2010. Origin of nutrients in Amazonian Anthrosols as assessed from 5 β -stanols, Sixth World Archaeological Congress, Dublin, pp. 145.
- Birk, J.J., Teixeira, W.G., Neves, E.G., Glaser, B., 2011. Faeces deposition on Amazonian Anthrosols as assessed from 5 β -stanols. *J Archaeol Sci* 38(6), 1209-1220.
- Bollyn, J., Faes, J., Fritzsche, A., Smolders, E., 2017. Colloidal-Bound Polyphosphates and Organic Phosphates Are Bioavailable: A Nutrient Solution Study. *J Agr Food Chem* 65(32), 6762-6770.
- Brodowski, S., Rodionov, A., Haumaier, L., Glaser, B., Amelung, W., 2005. Revised black carbon assessment using benzene polycarboxylic acids. *Organic Geochemistry* 36(9), 1299-1310.
- Bull, I.D., Lockheart, M.J., Elhmmali, M.M., Roberts, D.J., Evershed, R.P., 2002. The origin of faeces by means of biomarker detection. *Environ Int* 27(8), 647-654.
- Cade-Menun, B., Preston, C., 1996. A comparison of soil extraction procedures for ³¹P NMR spectroscopy. *Soil Sci.* 161(11), 770-785.
- Cade-Menun, B.J., 2015. Improved peak identification in P-31-NMR spectra of environmental samples with a standardized method and peak library. *Geoderma* 257, 102-114.
- Carstens, J.F., Bachmann, J., Neuweiler, I., 2018. Effects of organic matter coatings on the mobility of goethite colloids in model sand and undisturbed soil. *Eur. J. Soil Sci.* 69(2), 360-369.
- Chia, C.H., Munroe, P., Joseph, S.D., Lin, Y., Lehmann, J., Muller, D.A., Xin, H.L., Neves, E., 2012. Analytical electron microscopy of black carbon and microaggregated mineral matter in Amazonian dark Earth. *Journal of Microscopy* 245(2), 129-139.
- Chorover, J., Amistadi, M.K., Chadwick, O.A., 2004. Surface charge evolution of mineral-organic complexes during pedogenesis in Hawaiian basalt. *Geochim. Cosmochim. Acta* 68(23), 4859-4876.
- Cornelissen, G., Gustafsson, O., Bucheli, T.D., Jonker, M.T.O., Koelmans, A.A., Van Noort, P.C.M., 2005. Extensive sorption of organic compounds to black carbon, coal, and

- kerogen in sediments and soils: Mechanisms and consequences for distribution, bioaccumulation, and biodegradation. *Environ. Sci. Technol.* 39(18), 6881-6895.
- da Costa, M.L., Kern, D.C., 1999. Geochemical signatures of tropical soils with archaeological black earth in the Amazon, Brazil. *J Geochem Explor* 66(1), 369-385.
- da Costa, M.L., Kern, D.C., Kämpf, N., 2003. Pedogeochemical and mineralogical analyses of Amazonian Dark Earths, Amazonian Dark Earths. Springer, pp. 333-351.
- Davari, M., Gholami, L., Nabiollahi, K., Homaei, M., Jafari, H.J.J.S., Research, T., 2020. Deforestation and cultivation of sparse forest impacts on soil quality (case study: West Iran, Baneh). 198, 104504.
- Falcão, N., Clement, C., Tsai, S., Comerford, N., 2009. Pedology, fertility, and biology of central Amazonian Dark Earths. *Amazonian Dark Earths: Wim Sombroek's Vision*, 213-228.
- Glaser, B., 1999. Eigenschaften und Stabilität des Humuskörpers der "Indianerschwarzherden" Amazoniens. Lehrstuhl für Bodenkunde und Bodengeographie der Univ.
- Glaser, B., 2007. Prehistorically modified soils of central Amazonia: a model for sustainable agriculture in the twenty-first century. *Philos. Trans. R. Soc. B-Biol. Sci.* 362(1478), 187-196.
- Glaser, B., Balashov, E., Haumaier, L., Guggenberger, G., Zech, W., 2000. Black carbon in density fractions of anthropogenic soils of the Brazilian Amazon region. *Organic Geochemistry* 31(7-8), 669-678.
- Glaser, B., Birk, J.J., 2012. State of the scientific knowledge on properties and genesis of Anthropogenic Dark Earths in Central Amazonia (terra preta de Indio). *Geochim. Cosmochim. Acta* 82, 39-51.
- Glaser, B., Guggenberger, G., Zech, W., 2004. Identifying the pre-Columbian anthropogenic input on present soil properties of Amazonian dark earths (terra preta). *Amazonian Dark Earths: Explorations in Space and Time*, 145-158.
- Glaser, B., Guggenberger, G., Zech, W., Ruivo, M.D.L., 2003. Soil organic matter stability in Amazonian Dark Earths, Amazonian Dark Earths. Springer, pp. 141-158.
- Glaser, B., Haumaier, L., Guggenberger, G., Zech, W., 1998. Black carbon in soils: the use of benzenecarboxylic acids as specific markers. *Organic Geochemistry* 29(4), 811-819.
- Glaser, B., Haumaier, L., Guggenberger, G., Zech, W., 2001. The 'Terra Preta' phenomenon: a model for sustainable agriculture in the humid tropics. *Naturwissenschaften* 88(1), 37-41.
- Gottselig, N., Amelung, W., Kirchner, J.W., Bol, R., Eugster, W., Granger, S.J., Hernandez-Crespo, C., Herrmann, F., Keizer, J.J., Korkiakoski, M., Laudon, H., Lehner, I., Lofgren, S., Lohila, A., Macleod, C.J.A., Molder, M., Muller, C., Nasta, P., Nischwitz,

- V., Paul-Limoges, E., Pierret, M.C., Pilegaard, K., Romano, N., Sebastia, M.T., Stahli, M., Voltz, M., Vereecken, H., Siemens, J., Klumpp, E., 2017. Elemental Composition of Natural Nanoparticles and Fine Colloids in European Forest Stream Waters and Their Role as Phosphorus Carriers. *Glob. Biogeochem. Cycle* 31(10), 1592-1607.
- Guggenberger, G., Christensen, B.T., Rubaek, G., Zech, W., 1996. Land-use and fertilization effects on P forms in two European soils: Resin extraction and P-31-NMR analysis. *Eur J Soil Sci* 47(4), 605-614.
- Gustafsson, J.P., Mwamila, L.B., Kergoat, K., 2012. The pH dependence of phosphate sorption and desorption in Swedish agricultural soils. *Geoderma* 189, 304-311.
- Hammes, K., Smernik, R.J., Skjemstad, J.O., Herzog, A., Vogt, U.F., Schmidt, M.W.I., 2006. Synthesis and characterisation of laboratory-charred grass straw (*Oryza saliva*) and chestnut wood (*Castanea sativa*) as reference materials for black carbon quantification. *Organic Geochemistry* 37(11), 1629-1633.
- Hathaway, J.C., 1956. Procedure for clay mineral analysis used in the sedimentary petrology laboratory of the US Geological Survey. *Clay minerals bulletin* 3, 8-13.
- Haygarth, P.M., Warwick, M.S., House, W.A., 1997. Size distribution of colloidal molybdate reactive phosphorus in river waters and soil solution. *Water Res* 31(3), 439-448.
- Hussain, M.Z., Robertson, G.P., Basso, B., Hamilton, S.K., 2020. Leaching losses of dissolved organic carbon and nitrogen from agricultural soils in the upper US Midwest. *Science of the Total Environment* 734, 10.
- Javidpour, J., Molinero, J.C., Lehmann, A., Hansen, T., Sommer, U., 2009. Annual assessment of the predation of *Mnemiopsis leidyi* in a new invaded environment, the Kiel Fjord (Western Baltic Sea): a matter of concern? *Journal of Plankton Research* 31(7), 729-738.
- Jiang, X., Bol, R., Willbold, S., Vereecken, H., Klumpp, E., 2015a. Speciation and distribution of P associated with Fe and Al oxides in aggregate-sized fraction of an arable soil. *Biogeosciences* 12(21), 6443-6452.
- Jiang, X.Q., Bol, R., Cade-Menun, B.J., Nischwitz, V., Willbold, S., Bauke, S.L., Vereecken, H., Amelung, W., Klumpp, E., 2017. Colloid-bound and dissolved phosphorus species in topsoil water extracts along a grassland transect from Cambisol to Stagnosol. *Biogeosciences* 14(5), 1153-1164.
- Jiang, X.Q., Bol, R., Nischwitz, V., Siebers, N., Willbold, S., Vereecken, H., Amelung, W., Klumpp, E., 2015b. Phosphorus Containing Water Dispersible Nanoparticles in Arable Soil. *J. Environ. Qual.* 44(6), 1772-1781.
- Kaiser, K., Guggenberger, G., Haumaier, L., 2003. Organic phosphorus in soil water under a European beech (*Fagus sylvatica* L.) stand in northeastern Bavaria, Germany: seasonal variability and changes with soil depth. *Biogeochemistry* 66(3), 287-310.

- Kappenberg, A., Blaesing, M., Lehndorff, E., Amelung, W., 2016. Black carbon assessment using benzene polycarboxylic acids: Limitations for organic-rich matrices. *Organic Geochemistry* 94, 47-51.
- Kern, D.C., d'Aquino, G., Rodrigues, T.E., Frazão, F.L., Sombroek, W., Myers, T.P., Neves, E.G., 2003. Distribution of Amazonian dark earths in the Brazilian Amazon. *Amazonian Dark Earths: origin, properties, management*, 51-75.
- Khormali, F., Ajami, M., Ayoubi, S., Srinivasarao, C., Wani, S.J.A., ecosystems, environment, 2009. Role of deforestation and hillslope position on soil quality attributes of loess-derived soils in Golestan province, Iran. 134(3-4), 178-189.
- Konrad, A., Billiy, B., Regenbogen, P., Bol, R., Lang, F., Klumpp, E., Siemens, J., 2020. Forest soil colloids enhance delivery of phosphorus into a Diffusive Gradient in Thin films (DGT) sink. *Front. For. Glob. Change*.
- Krause, L., Klumpp, E., Nofz, I., Missong, A., Amelung, W., Siebers, N., 2020. Colloidal iron and organic carbon control soil aggregate formation and stability in arable Luvisols. *Geoderma* 374, 13.
- Lehmann, J., Campos, C.V., De Macedo, J.L.V., German, L., 2004. Sequential P fractionation of relict anthropogenic Dark Earths of Amazonia, *Amazonian Dark Earths: Explorations in Space and Time*. Springer, pp. 113-123.
- Lehmann, J., da Silva, J.P., Steiner, C., Nehls, T., Zech, W., Glaser, B., 2003. Nutrient availability and leaching in an archaeological Anthrosol and a Ferralsol of the Central Amazon basin: fertilizer, manure and charcoal amendments. *Plant Soil* 249(2), 343-357.
- Lehmann, J., Lan, Z.D., Hyland, C., Sato, S., Solomon, D., Ketterings, Q.M., 2005. Long-term dynamics of phosphorus forms and retention in manure-amended soils. *Environ Sci Technol* 39(17), 6672-6680.
- Lespes, G., Gigault, J., Battu, S., 2015. Field Flow Fractionation. *Analytical Separation Science*.
- Liang, B., Lehmann, J., Solomon, D., Kinyangi, J., Grossman, J., O'Neill, B., Skjemstad, J.O., Thies, J., Luizao, F.J., Petersen, J., Neves, E.G., 2006. Black Carbon increases cation exchange capacity in soils. *Soil Sci. Soc. Am. J.* 70(5), 1719-1730.
- Lima, A.B., Muniz, A.W., Dumont, M.G., 2014. Activity and abundance of methane-oxidizing bacteria in secondary forest and manioc plantations of Amazonian Dark Earth and their adjacent soils. *Frontiers in microbiology* 5, 550.
- Lima, H.N., Schaefer, C.E.R., Mello, J.W.V., Gilkes, R.J., Ker, J.C., 2002. Pedogenesis and pre-Colombian land use of "Terra Preta Anthrosols" ("Indian black earth") of Western Amazonia. *Geoderma* 110(1), 1-17.
- Mann, C.C., 2002. The real dirt on rainforest fertility. *American Association for the Advancement of Science*.

- Marschner, B., Brodowski, S., Dreves, A., Gleixner, G., Gude, A., Grootes, P.M., Hamer, U., Heim, A., Jandl, G., Ji, R., Kaiser, K., Kalbitz, K., Kramer, C., Leinweber, P., Rethemeyer, J., Schaeffer, A., Schmidt, M.W.I., Schwark, L., Wiesenberger, G.L.B., 2008. How relevant is recalcitrance for the stabilization of organic matter in soils? *J. Plant Nutr. Soil Sci.* 171(1), 91-110.
- McDowell, R.W., Cade-Menun, B., Stewart, I., 2007. Organic phosphorus speciation and pedogenesis: analysis by solution P-31 nuclear magnetic resonance spectroscopy. *Eur J Soil Sci* 58(6), 1348-1357.
- McDowell, R.W., Stewart, I., 2005. Peak assignments for phosphorus-31 nuclear magnetic resonance spectroscopy in pH range 5-13 and their application in environmental samples. *Chem Ecol* 21(4), 211-226.
- Missong, A., Bol, R., Nischwitz, V., Krüger, J., Lang, F., Siemens, J., Klumpp, E., 2017. Phosphorus in water dispersible-colloids of forest soil profiles. *Plant Soil*, 1-16.
- Missong, A., Bol, R., Willbold, S., Siemens, J., Klumpp, E., 2016. Phosphorus forms in forest soil colloids as revealed by liquid-state P-31-NMR. *J. Plant Nutr. Soil Sci.* 179(2), 159-167.
- Missong, A., Holzmann, S., Bol, R., Nischwitz, V., Puhlmann, H., von Wilpert, K., Siemens, J., Klumpp, E., 2018a. Leaching of natural colloids from forest topsoils and their relevance for phosphorus mobility. *Science of the Total Environment* 634, 305-315.
- Missong, A., Schäffer, A., Klumpp, E., 2018b. Phosphorus associated to forest soil colloids, RWTH Aachen University.
- Montavo, D., Degryse, F., McLaughlin, M.J., 2015. Natural Colloidal P and Its Contribution to Plant P Uptake. *Environ Sci Technol* 49(6), 3427-3434.
- Oliveira, N.C., Paschoal, A.R., Paula, R.J., Constantino, I.C., Bisinoti, M.C., Moreira, A.B., Fregolente, L.G., Santana, A.M., Sousa, F.A., Ferreira, O.P., Paula, A.J., 2018. Morphological analysis of soil particles at multiple length-scale reveals nutrient stocks of Amazonian Anthrosols. *Geoderma* 311, 58-66.
- Perakis, S.S., Hedin, L.O., 2002. Nitrogen loss from unpolluted South American forests mainly via dissolved organic compounds. *Nature* 415(6870), 416-419.
- Ruivo, M.d.L.P., da Silva Cunha, E., Kern, D.C., 2004. Organic Matter in Archaeological Black Earths and Yellow Latosol in the Caxivanã, Amazonia, Brazil, Amazonian Dark Earths: Explorations in Space and Time. Springer, pp. 95-111.
- Saidy, A.R., Smernik, R.J., Baldock, J.A., Kaiser, K., Sanderman, J., 2013. The sorption of organic carbon onto differing clay minerals in the presence and absence of hydrous iron oxide. *Geoderma* 209-210, 15-21.
- Saidy, A.R., Smernik, R.J., Baldock, J.A., Kaiser, K., Sanderman, J., Macdonald, L.M., 2012. Effects of clay mineralogy and hydrous iron oxides on labile organic carbon stabilisation. *Geoderma* 173, 104-110.

- Schaefer, C., Gilkes, R., Fernandes, R., 2004. EDS/SEM study on microaggregates of Brazilian Latosols, in relation to P adsorption and clay fraction attributes. *Geoderma* 123(1-2), 69-81.
- Schimpf, M.E., Caldwell, K., Giddings, J.C., 2000. Field-flow fractionation handbook. John Wiley & Sons.
- Sombroek, W., Ruivo, M.D., Fearnside, P.M., Glaser, B., Lehmann, J., 2004. Amazonian Dark Earths as carbon stores and sinks. *Amazonian Dark Earths: Origin, Properties, Management*, 125-139.
- Steiner, C., Teixeira, W.G., Lehmann, J., Nehls, T., de Macedo, J.L.V., Blum, W.E.H., Zech, W., 2007. Long term effects of manure, charcoal and mineral fertilization on crop production and fertility on a highly weathered Central Amazonian upland soil. *Plant Soil* 291(1-2), 275-290.
- Stolpe, B., Guo, L.D., Shiller, A.M., Aiken, G.R., 2013. Abundance, size distributions and trace-element binding of organic and iron-rich nanocolloids in Alaskan rivers, as revealed by field-flow fractionation and ICP-MS. *Geochim. Cosmochim. Acta* 105, 221-239.
- Taketani, R.G., Lima, A.B., da Conceição Jesus, E., Teixeira, W.G., Tiedje, J.M., Tsai, S.M., 2013. Bacterial community composition of anthropogenic biochar and Amazonian anthrosols assessed by 16S rRNA gene 454 pyrosequencing. *Antonie van Leeuwenhoek* 104(2), 233-242.
- Tombácz, E., Libor, Z., Illes, E., Majzik, A., Klumpp, E.J.O.G., 2004. The role of reactive surface sites and complexation by humic acids in the interaction of clay mineral and iron oxide particles. *35(3)*, 257-267.
- Totsche, K.U., Amelung, W., Gerzabek, M.H., Guggenberger, G., Klumpp, E., Knief, C., Lehndorff, E., Mikutta, R., Peth, S., Pechtel, A., Ray, N., Kogel-Knabner, I., 2018. Microaggregates in soils. *J Plant Nutr Soil Sc* 181(1), 104-136.
- Turner, B.L., Engelbrecht, B.M., 2011. Soil organic phosphorus in lowland tropical rain forests. *Biogeochemistry* 103(1-3), 297-315.
- Turner, B.L., Mahieu, N., Condon, L.M., 2003. Phosphorus-31 nuclear magnetic resonance spectral assignments of phosphorus compounds in soil NaOH-EDTA extracts. *Soil Sci Soc Am J* 67(2), 497-510.
- Turrion, M.B., Lafuente, F., Aroca, M.J., Lopez, O., Mulas, R., Ruiperez, C., 2010. Characterization of soil phosphorus in a fire-affected forest Cambisol by chemical extractions and P-31-NMR spectroscopy analysis. *Sci Total Environ* 408(16), 3342-3348.
- von Lutzow, M., Kogel-Knabner, I., Ekschmitt, K., Matzner, E., Guggenberger, G., Marschner, B., Flessa, H., 2006. Stabilization of organic matter in temperate soils: mechanisms and their relevance under different soil conditions - a review. *Eur. J. Soil Sci.* 57(4), 426-445.

- Walton, C.R., Zak, D., Audet, J., Petersen, R.J., Lange, J., Oehmke, C., Wichtmann, W., Kreyling, J., Grygoruk, M., Jablonska, E., Kotowski, W., Wisniewska, M.M., Ziegler, R., Hoffmann, C.C., 2020. Wetland buffer zones for nitrogen and phosphorus retention: Impacts of soil type, hydrology and vegetation. *Science of the Total Environment* 727, 20.
- Wolf, M., Lehndorff, E., Wiesenberger, G.L.B., Stockhausen, M., Schwark, L., Amelung, W., 2013. Towards reconstruction of past fire regimes from geochemical analysis of charcoal. *Organic Geochemistry* 55, 11-21.
- Woods, W.I., Denevan, W.M., 2009. Amazonian dark earths: the first century of reports, Amazonian Dark Earths: Wim Sombroek's Vision. Springer, pp. 1-14.
- Woods, W.I., McCann, J., 2003. Soils and sustainability in the prehistoric new world. *Exploitation and Overexploitation in Societies Past and Present*, 143-157.
- WRB, I.W.G., 2015. World reference base for soil resources 2014, update 2015: International soil classification system for naming soils and creating legends for soil maps. Fao Rome, pp. 192.
- Yan, J.L., Jiang, T., Yao, Y., Lu, S., Wang, Q.L., Wei, S.Q., 2016. Preliminary investigation of phosphorus adsorption onto two types of iron oxide-organic matter complexes. *J. Environ. Sci.* 42, 152-162.
- Zhang, H.L., Elskens, M., Chen, G.X., Chou, L., 2019. Phosphate adsorption on hydrous ferric oxide (HFO) at different salinities and pHs. *Chemosphere* 225, 352-359.
- Zhang, J., Luijten, E., Grzybowski, B.A., Granick, S., 2017. Active colloids with collective mobility status and research opportunities. *Chemical Society Reviews* 46(18), 5551-5569.